



Proceedings of the 11th International Conference on Environmental Engineering, Science and Management

(Full Papers)

May 12, 2022 at Pathumwan Princess Hotel,
Krung Thep Maha Nakhon (Bangkok), Thailand
May 13, 2022 Online Conference

Driving Sustainable Environment by Research and Innovation

Editors

Thares Srisatit Wanpen Wirojanagud Chart Chiemchaisri Pensri Watchalayann
Pantawat Sampanpanish Srilert Chotpantarat Apisit Numprasanthai Penradee Chanpiwat



M H E S I
กระทรวงการอุดมศึกษา วิทยาศาสตร์ วิจัยและนวัตกรรม
Ministry of Higher Education, Science, Research and Innovation



กระทรวงพลังงาน
MINISTRY OF ENERGY



SCGP



13R3-03	Health Risk Assessment Related to Heavy Metals Contamination in Ginger: A Case Study in Yangon, Myanmar <u>May Ko Ko</u> and Pokkate Wongsasuluk	292
13R3-04	The Readiness of Thailand's Local Government Agency for Greenhouse Gase Measurement, Report and Verification System Wilasinee Yoochatchaval and <u>Tantham Usayapan</u>	299
13R3-05	Assessment of the Sanitation Situation in Birendranagar Municipality, Nepal <u>Saroj Malakar</u> , Suwanna Boontanon, Romanee Thongdara, Trakarn Prapaspong and Nawatch Surinkul	306
13R3-06	Life Cycle Assessment of Energy Consumption in Thai Manufacturing Industry and Environmental Impact Reduction Pathways through Energy Plans <u>Tassawan Jaitiang</u> and Natanee Vorayos	312
13R3-07	DBPs Formation by Chlorination and Chloramination of Raw Water and Treated Water at Short and Long Reaction Times <u>Krittaporn Sitham</u> , Suthatip Sinyoung and Charongpun Musikavong	320
13R3-08	A Comparison of Aluminum-based Coagulants for Reducing a High Turbidity and DOC in Raw Water from the Canal Narongrit singsuwan, Chanoknart ontong, Krittaporn Sitham, Charongpun Musikavong and <u>Suthatip Sinyoung</u>	327
13R3-09	Urban Green Space Inventory using Different Spatial Resolution Satellite Images: Practical notes in Bangkok <u>Can Trong Nguyen</u> and Amnat Chidthaisong	333
13R3-10	Environmental Improvement of Aluminium Beverage Cans in Thailand Using Life Cycle Assessment <u>Apaphorn Prempreeda</u> , Parncheewa Kositcharoenkul, Phylo Zaw Oo, Sujitra Vassanadumrongdee, Shabbir H. Gheewala and Trakarn Prapaspong	341
13R3-11	The Ability of Bio-sludge for Removal Cadmium (Cd^{2+}) Contaminated Synthetic Wastewater <u>Tanta Suriyawong</u> , Sasidhorn Buddhwong, Thanit Swasdisevi and Suntud Sirianuntapiboon	349
13R3-12	Application of Manganese Contaminated Sludge for Rice Cultivation <u>Nopparat Inprasit</u> , Sasidhorn Buddhwong, Thanit Swasdisevi and Suntud Sirianuntapiboon	355

Urban Green Space Inventory Using Different Spatial Resolution Satellite Images: Practical Notes in Bangkok

Can Trong Nguyen^{1,2}, Amnat Chidthaisong^{1,2*}

¹ The Joint Graduate School of Energy and Environment, King Mongkut's University of Technology Thonburi, Bangkok 10140, Thailand; ² Center of Excellence on Energy Technology and Environment (CEE), Ministry of Higher Education, Science, Research and Innovation, Bangkok 10140, Thailand

* E-mail: amnat_c@jgsee.kmutt.ac.th

ABSTRACT

Green space inventory is a necessary task of urban managers and planners to understand the current status of green space in each specific area and then plan better greening strategies. Remote sensing-based inventory is an efficient option that applies diverse satellite images in the inventory. Yet, using satellite images with different spatial resolutions may lead to uncertainty or error. In contrast, each satellite image has its limitations, such as covering time, pixel size, revisit cycle, and acquiring cost. This study examined the applicability of two free-of-charge satellite images from Landsat-8 (30 m) and Sentinel-2 (10 m) in green space inventory. It found a slight difference in total area and percentage between green spaces acquired from Landsat-8 and Sentinel-2. There is no statistical significance between these two data for total area, percentage, and even green space per capita (GSPC) via T-test analysis. However, the spatial patterns of green patches extracted by one satellite image are significantly different from another, such as aggregation, the distance among patches, largest patch, patch shape, and patch density. An area with more green spaces with dense distribution close together and form complex patches that will significantly increase the homogeneity in GSPC estimated from satellite image regardless of sensor type. The research findings will be a basis for research related to urban green space depending on available data and research objectives.

Keywords: green space inventory, satellite, Landsat-8, Sentinel-2, green space per capita, spatial pattern.

INTRODUCTION

Many cities worldwide have experienced rapid urban expansion during the past few decades, especially in the east, south, and southeast Asian regions [1]. Urban expansion is a transition associated with changes in land use/land cover (LULC). Natural landscapes, e.g., cropland, agricultural land, and other green spaces, have been gradually shrunk and occupied by urban infrastructures, built-up, and impervious surfaces. Urbanization is also one of the main culprits of local climate change [2,3], in which urban heat island (UHI)—a phenomenon of city temperature is always hotter than its surrounding rural areas [4], is the most well-known microclimate impact. Ultimately, it affects the outdoor air environment, energy consumption, human well-being, heat-related morbidity, and mortality [5–9].

Many studies worldwide have witnessed UHI at different levels along with the urban development process, especially in tropical climate regions [10]. Temperature increase in urban areas has a significantly positive relationship with urban expansion and negative with the vegetation density and water surfaces [11–14]. Therefore, the presence of vegetation in cities, regardless of the category and size, is an economical and eco-friendly solution to mitigate heat harshness in urban areas [15,16]. In addition, urban green space also plays a vital role in purifying the urban air environment by trapping dust on leaves and absorbing carbon dioxide (CO₂) during photosynthesis; shading and transpiration through the stomata reduce air temperature, among other invisible benefits.

Nevertheless, over-urbanization without long-term and insightful planning induces a severe shortage of urban green space in developing cities, especially in downtown districts. Instead of green space conservation, they prioritize limited urban land funds for infrastructures and houses. It is a great challenge for urban planners when they need to carry out renovation plans in already developed areas to ensure green space per capita (GSPC) suggested by WHO (World Health Organization) for a primary city (9 m²/person) or ideal city (50 m²/person). Therefore, green space inventory plays a vital role in locating, managing activities, and planning sustainable urban developments. However, the current inventories are mainly based on official data on public green spaces regulated by land use maps. It should be noticed that every green patch in the urban areas is a meaningful asset contributing to improving urban environments. Therefore, the past inventories

may lead to underestimating urban green space potential, whereas remote sensing-based inventory is able to identify every individual green patch in urban areas.

Landsat-8 and Sentinel-2 are the most widely used data for urban studies among the currently active optical sensors. Landsat-8 is the eighth generation of the Landsat program that has extended the Landsat mission continuously for more than 50 years. Landsat data archive is the most useful dataset for long-term studies such as forest changes, urbanization, and climate changes, which should be observed for decades [17]. In contrast, Sentinel-2 was an emerging satellite starting only in 2015, with relatively high spatiotemporal resolution compared to Landsat. It is the first free-of-charge optical remote sensing data at 10-meter resolution with diverse red-edge and near-infrared (NIR) bands. Therefore, it is potentially applicable in crop and vegetation monitoring and numerous applications at a relatively detailed scale [18]. In general, Landsat supports long-term studies and comparisons with historical time hooks, while Sentinel-2 greatly aids in improving the data quality in studies with similar objectives. A question has arisen about whether these two satellite imageries can be utilized in a single inventory of green space in different periods, and if so, under what circumstances.

Therefore, this study aims to examine the applicability of Landsat-8 and Sentinel-2 in green space inventory. The potential disparities are investigated from different views (i.e., among districts and inner districts versus rural counties) and various parameters such as total area, percentage, green space per capita, and landscape metrics.

METHODOLOGY

Study area

Bangkok is one of the megacities in Southeast Asia, where rapid urbanization has continued since the middle period of the twentieth century. It quickly develops and becomes a regional development center of economy and services. Like other cities, the thermal environment of Bangkok has been changed remarkably due to urban expansion with compact construction density (Figure 1) [3,19,20]. As a megacity of more than 10.2 million residents (2018) with a high population density [21], Bangkok is under many pressures to efficiently provide urban green spaces for its residents, although the city government has been planning many public green spaces projects.

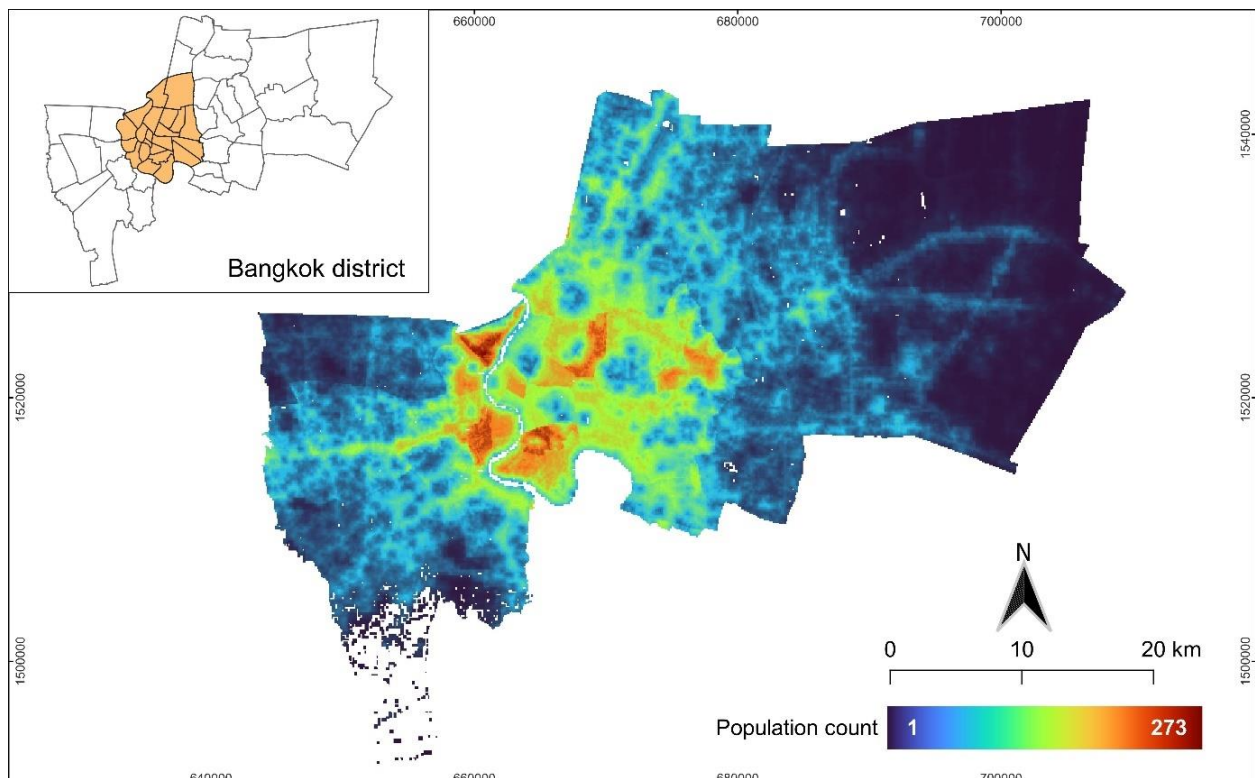


Figure 1 Study area in Bangkok highlights the city center and population counting data.

Data used

This study acquired satellite images from two medium-high spatial resolution sources of Landsat-8 at 30-meter resolution and Sentinel-2 at 10-meter resolution for urban green space detection. The images monitored during 2021 were filtered by the criteria of cloud cover rate (<5%) to ensure the data quality for further analyses. There were five scenes of Landsat-8 and 36 scenes of Sentinel-2 that passed the quality control step. The cloud and cloud shadow pixels on these images were then masked out before they were adopted to generate an annual composite image for each sensor. Finally, the annual composite was applied in this study to limit unwanted noises from seasonal vegetation such as cropland, upland vegetables, and rice fields. Besides, this research also acquired population data for estimating urban green space per capita (GSPC) [22,23]. This is one of the finest resolutions of the population data (100-km), estimated by integrating national data and estimated population from the United Nations.

Vegetation extraction

Vegetation layers used in this research were extracted using a remote sensing-based approach. Instead of classifying a comprehensive land use/land cover map with different land cover classes, we robustly extracted vegetation by thresholding method using the Normalized Difference Vegetation Index (NDVI) [24]. Although feature extraction using index images may achieve less accuracy compared to supervised classifier algorithms, it is proved to be efficient in single feature extraction (e.g., vegetation, bare soil, built-up) [25,26]. NDVI is based on plant biophysical phenology that Chlorophyll in healthy vegetation strongly absorbs visible wavelengths, and the cellular structure of the leaves strongly reflects near-infrared wavelength. Therefore, NDVI is determined by a ratio between visible red light (0.63 – 0.68 μm) and Near Infrared (0.78 – 0.89 μm). In addition to NDVI, we also involved Normalized Difference Water Index (NDWI) [27] to limit possible confusion caused by water features.

Firstly, water features on the considered site were detected for thresholding value, automatically estimated by Otsu's threshold optimal method [28]. The water thresholding values are approximately $\text{NDWI} = -0.083$ and $\text{NDWI} = 0.035$ for Landsat-8 and Sentinel-2, respectively. The water feature layer was adopted to mask out water features on NDVI images before they were used for vegetation detection by multi-Otsu's threshold (MOT)—it is also based on Otsu theory. The vegetation thresholding values for NDVI are about $\text{NDVI} = 0.327$ (Landsat-8) and $\text{NDVI} = 0.367$ (Sentinel-2).

Urban green space characteristics

Urban green space characteristics were calculated for each square shape with a 1-km edge covering the entire study site that was then used to compare the disparities between data extracted from Landsat-8 and Sentinel-2. These metrics consist of six standard parameters, which describe urban green space characteristics from different aspects. Specifically, PLAND (%) is a percentage of green spaces against total area; PD (patch/km²) is a ratio between a number of independent green patches and total green space area; ENN (meters) is Euclidean nearest neighbor distance or the shortest distance from a green patch to the nearest green patch based on edge-to-edge distance; AI (%) is aggregation index which represents an agglomeration of single patches into a clump or compact patch; LPI (%) is the largest patch size; and LSI (none unit) is landscape shape index—LSI describes the shape complexity of the green patch when considering its boundary shape.

Green space per capita estimation and comparison

Urban green space per capita was calculated for each square polygon as mentioned in Section 2.4. Each polygon was examined its total number of residents and corresponding green space for this polygon. GSPC is a ratio between total green space and total population.

The GSPC and landscape metrics were visualized and compared by independent T-test analysis to test whether the green space layers extracted from different satellite images will influence the urban green space inventory and evaluation. The null hypothesis (H_0) is that the average green spaces acquired from Landsat-8 and Sentinel-2 are equal; and the alternative hypothesis (H_1) is that the average green spaces obtained from these satellites are different. Besides, Pearson's correlation analysis was performed to identify the relationship between landscape metrics and the GSPC

RESULTS AND DISCUSSIONS

Urban green space availability

Remote sensing-based detection and inventory for green spaces are illustrated in Figure 2-a. Both Landsat-8 and Sentinel-2 are applicable in green space detection with high homogeneity among the two data sources. Specifically, the homogeneous green space areas detected by both data sources account for 64.8% of total green space areas. Landsat-8 identified a total area of 908.9 km² of green spaces, while Sentinel-2 detected a slightly smaller area, about 897.7 km². The comparison between green space areas in 50 districts for Landsat-8 and Sentinel-2 shows no statistical significance via T-test analysis ($p > 0.1$). When we considered the inner-urban and rural districts separately, it is obvious that the inner districts have fewer green spaces than rural districts, about 23 – 24% versus 52 – 53% (i.e., green space percentage variates due to sensor differences). Our assumption—sensor difference might significantly affect the inventory in the inner districts with small and scattered green patches, was not proven by the test. However, the statistical significance level (p -value) in the inner districts is relatively lower than in rural areas. It also implies that using different sensors might affect green space detection in the city center rather than in rural regions. Both the data sources are able to identify large and uniform patches (Figure 2-c), while Sentinel-2 tends to identify in more detail small green patches due to its finer pixel size (10 m) (Figure 2-b).

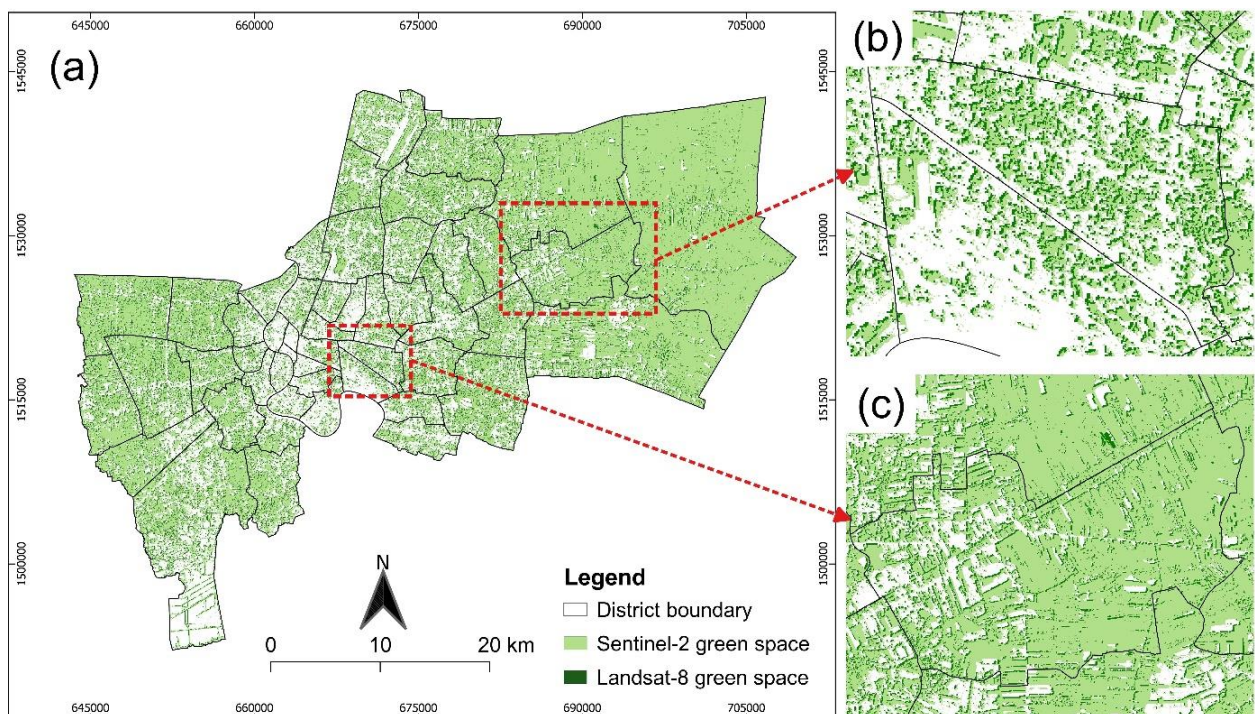


Figure 2 (a) Green spaces extracted from Landsat-8 and Sentinel-2 data entire Bangkok, (b) typical locations of sparse-small patches, and (c) large green space patches.

Urban green space patterns

Although there is no significant difference between the two sensors regarding the detectable area, the characteristics of green patches extracted from these data sources should deserve attention (Figure 3). As mentioned in the previous section, there is no significant disparity ($p = 0.717$) between green space density (PLAND), whether acquired from Landsat-8 or Sentinel-2 data. The general green proportion is about $40.3 \pm 19.76\%$ (Landsat-8) and $39.9 \pm 18.80\%$ (Sentinel-2).

Contrarily, the remaining five metrics revealed remarkable differences via T-test analysis ($p < 0.05$), when green spaces were retrieved by different sensors. In particular, the agglomeration of green patches was higher on Sentinel-based green spaces, $AI = 81.8 \pm 8.2\%$, while the patches on Landsat-8 were more disaggregated ($73.5 \pm 11.8\%$). Yet, when a certain region improves the aggregation of green spaces, i.e., green patches are gathered close together, the gap between the sensors is gradually narrowed and tends to have no great difference between them.

Sentinel-2 can detect more precisely the boundary of green patches due to its finer spatial resolution against Landsat-8, it is therefore able to recognize the more complicated shapes. The values of LSI for Sentinel-2

and Landsat-8 achieved 45.0 ± 15.0 and 22.2 ± 7.8 , respectively. Especially when the patch shape becomes more complex and irregular, the advantages of Sentinel-2 data over Landsat-8 are evident.

The most prominent characteristic we witnessed in the disparity between the sensors is patch density (PD). It is about 13.3 ± 7.1 patch/km² for Landsat-8, and 66.0 ± 28.0 patch/km² for Sentinel-2, a five-fold higher. This is also due to the pixel size difference that Sentinel-2 can locate small green patches with an actual area of 100 m². The mixed pixels of vegetation and other landscapes (e.g., bare soil, built-up, and wetland) may also be ignored on the coarse pixels of Landsat. Thus, the number of individual patches on Sentinel-2 is always much higher compared to those in Landsat. It then leads to higher PD calculated by Sentinel-2. Furthermore, Sentinel-2 is efficient in detecting small and scattered green patches; therefore, the distance among the green patches (ENN) estimated from Sentinel-2 is significantly shorter than Landsat; 28.9 ± 4.3 m versus 76.8 ± 11.2 m. In theory, LPI ranges from 0 to 100. The LPI value of 100 indicates that the entire considered region is totally covered by only one green patch, which is also the largest patch. The smaller values approaching zero mean the ratio of the largest patch against the total area in this region becomes smaller compared to the total region area. In general, Landsat-8 always tends to detect larger patches compared to Sentinel-2, which LPI is in turn about $20.8 \pm 21.6\%$ and $14.2 \pm 17.7\%$, respectively. The LPI is relatively unique in comparison to other metrics. We observed that there is a great difference in LPI between Landsat and Sentinel when the largest patch of green space is from ~10% to 50%. When the largest patch is too big or small (i.e., less than 10% or higher than 50%), it seems to have no difference between the two sensors.

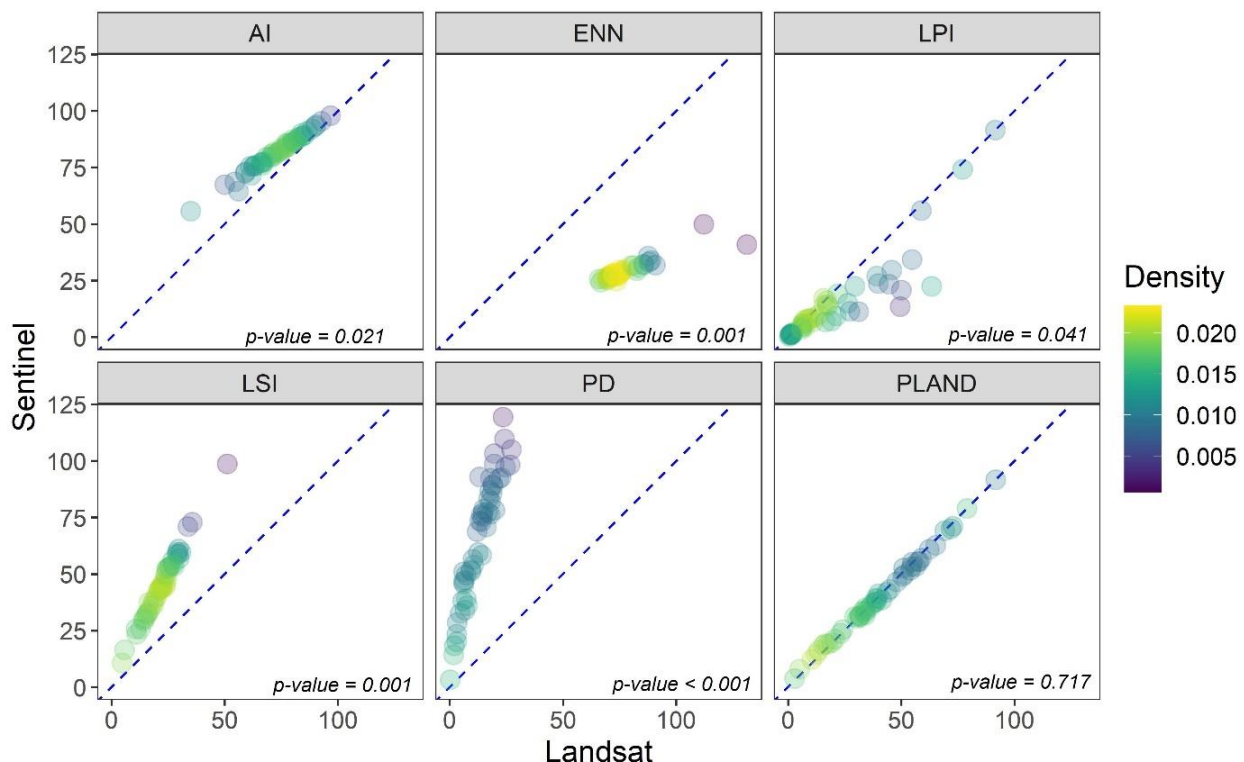


Figure 3 Landscape metrics comparison between Landsat-8 and Sentinel-2 for green space patches from district data.

Urban green space per capita and influential factors

Urban GSPC was estimated for 1-km grids corresponding to green spaces obtained from Landsat-8 and Sentinel-2. Figure 4 depicts GSPC from Sentinel-2 data and the difference between Landsat-8 and Sentinel-2. It is approximately $697.1 \pm 1,546.0$ m²/person (Landsat-8) and $686.2 \pm 1,488.2$ m²/person (Sentinel-2). Specifically, the GSPC in urban districts is about 804.8 m²/person and 792.2 m²/person for Landsat-8 and Sentinel-2, respectively. These numbers are only 23.5 m²/person (Landsat-8) and 23.7 m²/person (Sentinel-2). GSPC estimated from Landsat-8 is greater than Sentinel-2 in most cases except for urban inner districts where Sentinel-based GSPC is slightly higher than Landsat-8.

Regarding the spatial pattern of GSPC, most regions in Bangkok achieve the WHO standard of greater than $9.0 \text{ m}^2/\text{person}$ and the criteria for an ideal city ($>50 \text{ m}^2/\text{person}$), especially the peri-urban and rural regions outside the city center (Figure 4-a). On the other hand, the regions with a low capacity of green spaces are located in the city centers, such as Samphan Thawong ($<1 \text{ m}^2/\text{person}$), Pom Prap Sattru Phai (5.9 – 6.9 m^2/person), Bang Rak (8.5 – 8.8 m^2/person), Din Daeng (8.9 – 10.0 m^2/person).

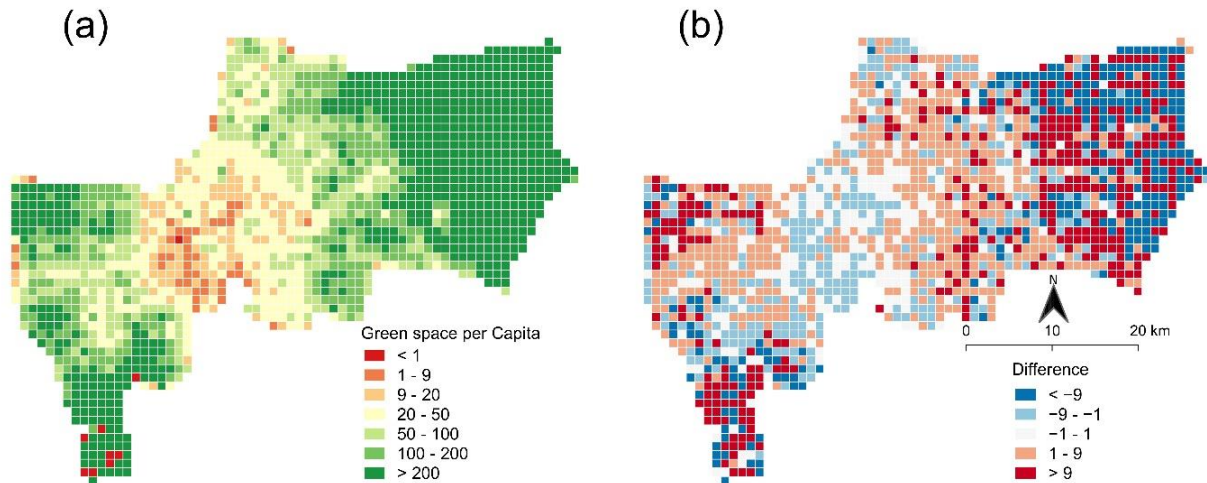


Figure 4 (a) Greenspace per capita estimated from Sentinel-based green spaces, and (b) difference in green space per capita between Landsat-8 and Sentinel-2.

The gap in GSPC between Landsat and Sentinel is shown in Figure 4-b. Specifically, most inner districts and suburban regions have small-medium gaps of about $\pm 9 \text{ m}^2/\text{person}$ —where there is less heterogeneity between the two data that could affect green space evaluation based on the WHO standard of $9 \text{ m}^2/\text{person}$. In comparison, the rural areas with high GSPC may get higher uncertainty ($> 9 \text{ m}^2/\text{person}$) when estimates from Landsat-8 instead of Sentinel-2.

The correlation between landscape metrics and the GSPC disparity between Landsat-8 and Sentinel-2 is described in Table 1. There are significant associations between the GSPC difference between Landsat and Sentinel and AI, LSI, PLAND (negative relationships), and LPI (positive relationship). It means that there is lower uncertainty in GSPC in a region with higher green space density (PLAND), large and uniform shape (LPI and LSI), and the green patches should be highly aggregated (AI). Otherwise, it may lead to uncertainty in GSPC estimation when using different satellite data.

Table 1 Correlation of green space per capita difference between Landsat-8 and Sentinel-2 and landscape metrics.

Landscape metrics	AI	ENN	LSI	LPI	PD	PLAND
Correlation coefficient (R)	-0.044	0.013	-0.050	0.054	-0.017	-0.069
p-value	0.071 ⁺	0.602	0.039*	0.028*	0.495	0.005**

Notes: Significance level (2-tailed): *** is $p < 0.001$; ** is $p < 0.01$; * is $p < 0.05$; + is $p < 0.1$

CONCLUSION

The green space inventory based on the remote sensing approach from Landsat-8 and Sentinel-2 imageries was adopted in this empirical study. Using a consistent methodological workflow to extract green spaces from NDVI and Otsu's threshold, our study identified about $897.7 - 908.2 \text{ km}^2$ of green spaces for the entire Bangkok metropolitan in 2021. Greenspace data acquired from Landsat-8 is relatively larger than that was obtained from Sentinel-2 because Sentinel-2 can detect the green patch and its boundary with relatively high resolution. The gaps in the area between the two data among the districts are relatively small and insignificant. It is similar to GSPC data when the differences between Landsat-8 and Sentinel-2 data have not been found. However, it should be noticed that the disparity may be increasingly greater in urban districts

with limited green spaces. We also need an official data source of spatial green spaces to verify which sensor performs better inventory in terms of spatial distribution and area before a recommendation is stated.

Although no statistically significant disparity was found between the two sensors regarding the accumulative area, distribution, and GSPC, a few other spatial characteristics should be concerned when using one sensor instead of another. With finer pixel size, Sentinel-2 data generates green space data with high agglomeration, the low shortest distance among patches, and small green patches against Landsat-8. Especially, the shape and density of patches are remarkably higher in Sentinel-2 data when it is able to detect more small patches with small length edges that could not be described by the coarse pixel of Landsat-8. These spatial patterns were proven to significantly influence the value gaps of GSPC between the sensors in an area with fewer, sparse, and scattered vegetation. Hence, if the users aim to quantitatively inventory for green space availability and GSPC, the sensor type will have little effect on the outputs. Yet, to identify green space characteristics, which is essential in evaluating the cooling effect of urban green spaces [29], the sensor type, especially in the city center, should be taken into account.

ACKNOWLEDGEMENT

The authors sincerely thank Petchra Pra Jom Klae Doctoral Scholarship, King Mongkut's University of Technology Thonburi, Joint Graduate School of Energy and Environment (JGSEE), and the Center of Excellence on Energy Technology and Environment (CEE), Ministry of Higher Education, Science, Research and Innovation for financial supports to accomplish this research. Our gratitude is expressed to all data providers (WorldPop, United States Geological Survey, and Google Earth Engine) for the data used in this study.

REFERENCE

- [1] Yamashita, A. Rapid Urbanization in Developing Asia and Africa. In: Murayama, Y., Kamusoko, C., Yamashita, A., Estoqe, R.C. *Urban Development in Asia and Africa Geospatial Analysis of Metropolises*, Springer Nature Singapore, 2017; 47–61.
- [2] Estoqe, R.C., Murayama, Y. 2017. Monitoring surface urban heat island formation in a tropical mountain city using Landsat data (1987–2015). *ISPRS Journal of Photogrammetry and Remote Sensing*. 133: 18–29.
- [3] Khamchiangta, D., Dhakal, S. 2019. Physical and non-physical factors driving urban heat island: Case of Bangkok Metropolitan Administration, Thailand. *Journal of Environmental Management*. 248: 109285
- [4] US EPA. 2008. *Urban Heat Island Basics*. U.S. Environmental Protection Agency, Washington, DC.
- [5] Arifwidodo, S.D., Chandrasiri, O., Abdulharis, R., Kubota, T. 2019. Exploring the effects of urban heat island: A case study of two cities in Thailand and Indonesia. *APN Science Bulletin*. 9(1): 10–18.
- [6] Lowe, S.A. 2016. An energy and mortality impact assessment of the urban heat island in the US. *Environmental Impact Assessment Review*. 56: 139–144.
- [7] Santamouris, M. 2020. Recent progress on urban overheating and heat island research. Integrated assessment of the energy, environmental, vulnerability and health impact: Synergies with the global climate change. *Energy and Buildings*. 207: 109482.
- [8] Mashhoodi, B., Stead, D., van Timmeren, A. 2020. Land surface temperature and households' energy consumption: Who is affected and where? *Applied Geography*. 114: 102125.
- [9] Nguyen, C.T., Diep, N.T.H., Diem, P.K. 2021. Factors affecting urban electricity consumption: a case study in the Bangkok Metropolitan Area using an integrated approach of earth observation data and data analysis. *Environmental Science and Pollution Research*. 28: 12056–12066.
- [10] Chapman, S., Watson, J.E.M., Salazar, A., Thatcher, M., McAlpine, C.A. 2017. The impact of urbanization and climate change on urban temperatures: a systematic review. *Landscape Ecology*. 32(10): 1921–1935.
- [11] Can, N.T., Diep, N.T.H., Iabchoon, S., Varnakovida, P., Minh, V.Q. 2019. Analysis of Factors Affecting Urban Heat Island Phenomenon in Bangkok Metropolitan Area, Thailand. *VNU Journal of Science: Earth and Environmental Sciences*. 35(1): 53–62.
- [12] Yaung, K. L., Chidthaisong, A., Limsakul, A., Varnakovida, P., Can, N.T. 2021. Land Use Land Cover Changes and Their Effects on Surface Air Temperature in Myanmar and Thailand. *Sustainability*. 13(19): 1–21.

- [13] Yang, Z., Witharana, C., Hurd, J., Wang, K., Hao, R., Tong, S. 2020. Using Landsat 8 data to compare percent impervious surface area and normalized difference vegetation index as indicators of urban heat island effects in Connecticut, USA. *Environmental Earth Sciences*. 79(18): 1–13.
- [14] Xinmin, Z., Estoqe, R.C., Murayama, Y. 2017. An urban heat island study in Nanchang City, China based on land surface temperature and social-ecological variables. *Sustainable Cities and Society*. 32: 557–568.
- [15] Aram, F., García, E. H., Solgi, E., Mansournia, S. 2019. Urban green space cooling effect in cities. *Heliyon*. 5(4): e01339.
- [16] Aflaki, A., Mirnezhad, M., Ghaffarianhoseini, A., Ghaffarianhoseini A., Omrany, H., Wang, Z.H., Akbari, H. 2017. Urban heat island mitigation strategies: A state-of-the-art review on Kuala Lumpur, Singapore and Hong Kong. *Cities*. 62: 131–145.
- [17] Wulder, M.A., Loveland, T.R., Roy, D.P., Crawford, C.J., Masek, J.G., Woodcock, C.E., Allen, R.G., Anderson, M.C., Belward, A.S., Cohen, W.B., Dwyer, J., Erb, A., Gao, F., Griffiths, P., Helder, D., Hermosilla, T., Hipple, J.D., Hostert, P., Hughes, M.J., Huntington, J., Johnson, D.M., Kennedy, R., Kilic, A., Li, Z., Lymburner, L., McCorkel, J., Pahlevan, N., Scambos, T.A., Schaaf, C., Schott, J.R., Sheng, Y., Storey, J., Vermote, E., Vogelmann, J., White, J.C., Wynne, R.H., Zhu, Z. 2019. Current status of Landsat program, science, and applications. *Remote Sensing of Environment*. 225: 127–147.
- [18] Phiri, D., Simwanda, M., Salekin, S., Ryirenda, V.R., Murayama, Y., Ranagalage, M., Oktaviani, N., Kusuma, H.A., Zhang, T., Su, J., Liu, C., Chen, W.H., Liu, H., Liu, G., Cavur, M., Duzgun, H.S., Kemec, S., Demirkan, D.C., Chairet, R., Ben Salem, Y., Aoun, M., Kiala, Z., Mutanga, O., Odindi, J., Peerbhay, K. 2020. Sentinel-2 Data for Land Cover/Use Mapping: A Review. *Remote Sensing*. 12(14): 1–35.
- [19] Estoqe, R.C., Murayama, Y., Myint, S.W. 2017. Effects of landscape composition and pattern on land surface temperature: An urban heat island study in the megacities of Southeast Asia. *Science of the Total Environment*. 577: 349–359.
- [20] Srivanit, M. 2012. Assessing the Impact of Urbanization on Urban Thermal Environment: A Case Study of Bangkok Metropolitan. *International Journal of Applied Science and Technology*. 2(7): 243–256.
- [21] United Nations. 2018. The World's Cities in 2018: Data Booklet. Population Division, Department of Economic and Social Affairs, United Nations, New York.
- [22] WorldPop. 2018. Global High Resolution Population Denominators Project.
- [23] Gaughan, A.E., Stevens, F.R., Linard, C., Jia, P., Tatem, A.J. 2013. High Resolution Population Distribution Maps for Southeast Asia in 2010 and 2015. *PLoS One*. 8(2): e55882.
- [24] Tucker, C.J. 1979. Red and photographic infrared linear combinations for monitoring vegetation. *Remote Sensing of Environment*. 8(2): 127–150.
- [25] Nguyen, C.T., Chidthaisong, A., Diem, P.K., Huo, L. 2021. A Modified Bare Soil Index to Identify Bare Land Features during Agricultural Fallow-Period in Southeast Asia Using Landsat 8. *Land*. 10(231): 1–17.
- [26] Mzid, N., Pignatti, S., Huang, W., Casa, R. 2021. An analysis of bare soil occurrence in arable croplands for remote sensing topsoil applications. *Remote Sensing*. 13(3): 1–24.
- [27] McFeeters, S.K. 1996. The use of the Normalized Difference Water Index (NDWI) in the delineation of open water features. *International journal of Remote sensing*. 17(7): 1425–1432.
- [28] Otsu, N. 1979. A Threshold Selection Method from Gray-Level Histograms. *IEEE Transactions on Systems, Man, and Cybernetics*. 9(1): 62–66.
- [29] Maimaitiyiming, M., Ghulam, A., Tiyip, T., Pla, F., Latorre-Carmona, P., Halik, Ü., Sawut, M., Caetano, M. 2014. Effects of green space spatial pattern on land surface temperature: Implications for sustainable urban planning and climate change adaptation. *ISPRS Journal of Photogrammetry and Remote Sensing*. 89: 59–66.